Intrinsic Quantum Efficiencies of Semiconductor Photoelectrodes Obtained by Temperature Measurement

Akira FUJISHIMA,* Yasuhisa MAEDA, and Kenichi HONDA

Department of Synthetic Chemistry, Faculty of Engineering, The University of Tokyo, Hongo, Bunkyo-ku, Tokyo 113

(Received February 20, 1980)

Quantum efficiencies of photoelectrochemical reactions on n-type and p-type semiconductor electrodes can easily be determined by the measurement of temperature changes of the surface of semiconductor electrodes by use of thermistors. The quantum efficiencies are intrinsic, since only the absorbed light quanta contribute to temperature change. The merits of the method, simplicity and applicability to the semiconductor of large surface reflectance, are discussed. The intrinsic quantum efficiencies were compared with those obtained by the usual chemical actinometric method.

Photothermal spectroscopy (PTS), a new spectroscopic method, has recently been developed.[1] A thermistor is placed on or close to a sample, and the temperature changes *i.e.*, thermistor resistance changes are measured during the course of irradiation of the sample with monochromatic light. It was found that the temperature change caused by light absorption is in line with the results of optical absorption spectroscopy. The method is applicable to cases in which samples are metal and semiconductor electrodes.[2-4]

A number of photoelectrochemical cells with use of semiconductor electrodes have been reported for the photodecomposition of water and the conversion of solar energy into electricity.[5-10] The energy conversion efficiencies and quantum efficiencies of electrochemical photocells are important for effective utilization of solar energy. Thermal measurements of semiconductor electrodes during the course of electrolysis facilitate the determination of the efficiencies.[4]

During the course of photoelectrochemical reaction only a portion of the light energy absorbed by the semiconductor can be utilized in the electrode reaction.[11] The remaining portion of energy is exhausted as heat. Thus, the efficiency of the process can be studied by monitoring temperature changes at the photoelectrodes as a function of electrode potential. In a previous paper, experimental results obtained by using CdS and TiO_2 single crystal photoanodes were presented, interpretation being given by means of a model for the energy balance within the system. The quantum efficiency and power efficiency could be determined without calibration of the irradiation source. The equation was derived by considering the energy balance within a semiconductor photoelectrode.[4] Let us consider the case in which the semiconductor electrode is illuminated with a monochromatic light pulse having an energy E (eV/photon), with an average absorbed intensity I (photon/s) for time t (s). The incoming energy (EIt) can then either be consumed by the semiconductor to promote the electrode reaction with the production of electric work (Vit) or evolved as heat in the semiconductor ($Q_{s.c.}$) *via* recombination and radiationless processes.

Thus the final equation for the overall photoelectrochemical reaction in the limiting photocurrent region is

$$E\frac{\Delta T}{\Delta T^\circ} = \frac{Q_{s.c.} + T\Delta S}{It} + e\eta_q(V - V_{fb}), \qquad (1)$$

where

ΔT: temperature change of the semiconductor surface
ΔT°: temperature change of the semiconductor surface in the open circuit
ΔS: entropy change for the semiconductor electrode reaction
$Q_{s.c.}$: heat evolved in the semiconductor *via* recombination and radiationless processes
$\eta_q\left(=\frac{i}{I}\right)$: quantum efficiency of photo-electrode reaction
V: applied potential (V *vs.* reference electrode)
V_{fb}: flatband potential (V *vs.* reference electrode).

Thus under constant illumination conditions (constant EIt) the plot $E\frac{\Delta T}{\Delta T^\circ}$ *vs.* $(V - V_{fb})$ gives the quantum efficiency, η_q, from the slope of the straight line and the loss term, $\frac{Q_{s.c.} + T\Delta S}{It}$, is obtained from the intercept of the $E\frac{\Delta T}{\Delta T^\circ}$ axis at $V = V_{fb}$ as shown in Fig. 1.

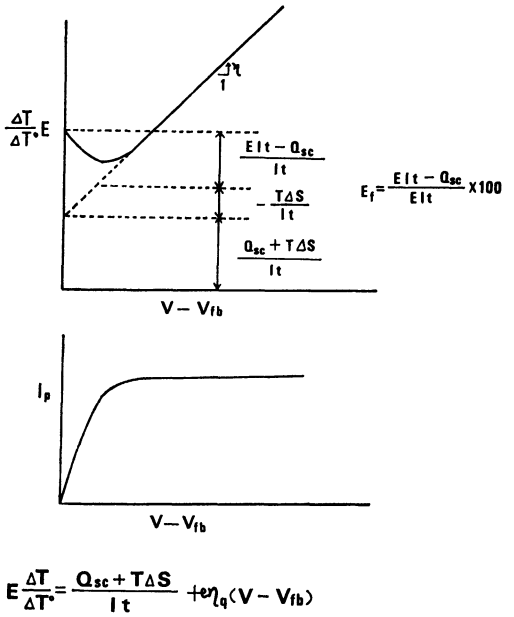

Fig. 1. Theoretical behavior of the temperature change *versus* potential.

From the loss term $\frac{Q_{s.c.} + T\Delta S}{It}$ the energy conversion efficiency

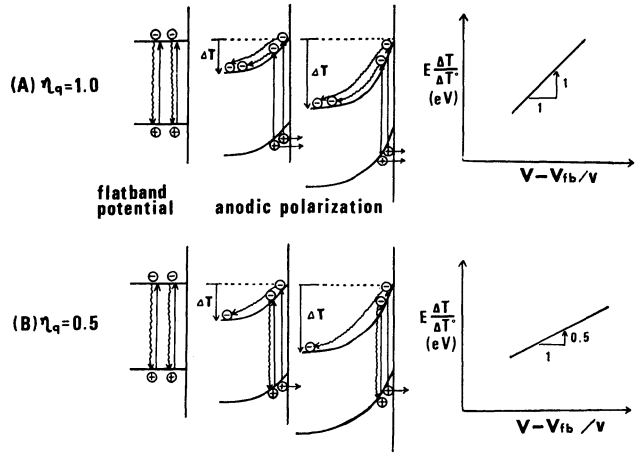

Fig. 2. Relationship between the temperature change and the applied potential in two model cases ((A), (B)). (A): Quantum efficiency is 1.0, (B): quantum efficiency is 0.5.

$$\eta_e = \frac{EIt - Q_{s.c.}}{EIt} \quad (2)$$

can be easily obtained by making appropriate correction for the entropy change $T\Delta S$ associated with the electrode reaction.

In order to illustrate the use of Eq. 1 for obtaining quantum efficiency, two model cases are given (Fig. 2). When $\eta_q=1.0$, the slope of $E\frac{\Delta T}{\Delta T^\circ}$ against V should be 1.0, since all the electrons excited into the conduction band by light irradiation move from the surface into the bulk of the semiconductor through the space charge layer giving rise to heat generation. When $\eta_q=0.5$, the slope should be 0.5, since half of the excited electrons are recombined with the holes in the surface region.

Determination of the quantum efficiencies of various photoelectrodes [semiconductors of n-type (CdS, CdSe, GaP, GaAs, ZnO, TiO_2, and MoS_2), and p-type (GaP and GaAs)] can easily be carried out by direct measurement of temperature changes in the semiconductor electrodes.

Experimental

Procedure. The photothermal experiment on the photoelectrodes made of single crystals or polycrystals of n-CdS, n-CdSe, n-GaP, n-GaAs, n-TiO_2, n-ZnO, n-MoS_2, p-GaP, and p-GaAs (Table 1) was carried out according to the method reported.[4] Results are given for monochromatic irradiation at wavelengths shorter than that corresponding to the band gap energy (*e.g.* 340 nm for CdS). Photothermal responses were obtained for the photoelectrodes during anodic (n-type semiconductor) or cathodic (p-type) polarization, and under open circuit conditions in the electrolyte solutions. The corresponding current and temperature changes were then plotted as a function of potential *vs.* flatband potential or applied potential.

Apparatus. A block diagram of the apparatus is shown in Fig. 3. The light source employed was a 500 W high pressure mercury lamp (Ushio Electric) in an Ushio Model UI-501C lamp house. A lens to focus the light beam, interference filters (Koshin Kogaku) to select the wavelength of the exciting light, and a shutter with two timers (Ishikawa Seisakusho) to fix the irradiation period precisely were used.

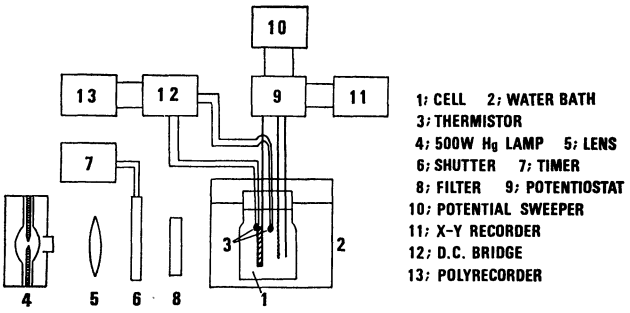

Fig 3. Measurement assembly.

The current-potential and current-time curves were measured under potentiostatic conditions with a potentiostat and a potential programmer (Nikko Keisoku, Models NPGS-301 and NPS-2). Cyclic voltammograms and current-time curves were displayed on an X-Y recorder (Yokokawa, Type 3078).

Characteristics of the semiconductor electrodes are given in Table 1. After ohmic contact, a copper wire was attached to the contact with conducting silver epoxy (Seisin Shoji, No. 4922). The back and sides of the crystal were insulated and mounted on a flat piece of glass attached to a glass rod with epoxy resin (Cemedain).

In order to measure the temperature changes, we used matched pairs of thermistors (Shibaura Electronics, Model BSB4-41A; nominal resistance 4 K Ω, sensitivity 0.052 °C/Ω). The thermistors having a time constant 0.4 s when immersed in still water were used in a differential arrangement with one held against the front surface of the semiconductor electrode and the other placed behind the electrode but not touching it. The cell was placed so that the monochromatic light beam struck only the electrode and none of the thermistors. Thus a change in temperature of the electrode caused a resistive change in the thermistor, producing a voltage imbalance in the DC bridge. The small voltage was amplified and then displayed on a strip chart recorder (Toa Electronics, Model EPR-2T).

The monochromatic light intensity was measured accurately in order to know the usual quantum efficiencies of the photoelectrodes using a chemical actinometric method (potassium ferrioxalate).[12]

All chemicals were of reagent grade and used without further purification. Where necessary, prepurified nitrogen gas was bubbled through the solution in order to remove dissolved oxygen.

Results and Discussion

CdS-Na_2SO_3 System. $E\frac{\Delta T}{\Delta T^\circ}$ was plotted against $(V-V_{fb})$ for an illuminated CdS single crystal electrode in a sodium sulfite aqueous solution in accordance with Eq. 1, where illumination conditions are constant [I: constant, E: 340 nm (3.6 eV), t: 20 s] (Fig. 4).

From the intercept of the y axis obtained by extrapolating the linear portion of the curve to the flatband potential, the energy conversion efficiency of the photoelectrode can be calculated if the heat evolved in terms of an entropy change ($T\Delta S$) attributable to the electrode reaction is obtained.[13] Though the heat

Table 1. Semiconductor electrodes employed

Semiconductor	Single or polycrystal	Manufacture	Shape dimensions /mm³	Surface oriented	Carrier density /cm⁻³	Ohmic contact	Surface treatment
n-CdS	Single	Teikoku Tsushin	$10\times10\times1$	(001)	4.8×10^{16}	In–Ga alloy	Polished with 0.3 μm[a] alumina powder; immersed for 10 s in concd HCl
n-CdS[b]	Poly		Disk $15\phi\times1.5$			In–Ga alloy	Immersed for 10 s in concd HCl
n-CdSe	Single		$10\times10\times1$			In–Ga alloy	Polished with 0.3 μm alumina powder; immersed for 10 s in concd HCl
n-GaP	Single	Sumitomo Metal Mining	Surface area 120 mm²	(111)	4.6×10^{17} (top) 1.1×10^{18} (bottom)	Au–Ge alloy evaporated; and heating in H_2 at 600 °C for 10—15 min	Polished with 0.3 μm[c] alumina powder; immersed for 30 s in aqua regia
n-GaAs	Single	Mitsubishi Metal	$10\times20\times1$	(100)	2.1×10^{17}	Au–Ge alloy evaporated; and heating at 600 °C for 10 min	Polished with 0.3 μm[d] alumina powder; immersed for 30 s in mixture of concd H_2SO_4, 30% H_2O_2, H_2O (3:1:1)
n-TiO_2	Single	Nakazumi Crystal	$15\times15\times1.5$	(001)		In–Ga alloy	Polished with 0.3 μm alumina powder; immersed for 10 s in concd H_2SO_4
n-ZnO[e]	Poly		Disk $15\phi\times1.5$			In–Ga alloy	Immersed for 10 s[f] in concd HCl
n-MoS_2	Single	Iwamoto Kobutsu	$10\times10\times10$	C axis	about[g] 1.3×10^{18}	In–Ga alloy	Immersed for 30 s[h] in 2 M HCl
p-GaP	Single	Sumitomo Metal Mining	Surface area 170 mm²	(100)	2.1×10^{17} (top) 3.5×10^{17} (bottom)	Au–Zn alloy evaporated; and heating in H_2 at 600 °C for 10—15 min	Polished with 0.3 μm[c] alumina powder; immersed for 30 s in aqua regia
p-GaAs	Single	Mitsubishi Metal	Surface area 150 mm²	(100)	3.34×10^{16} (front) 1.6×10^{17} (back)	Au evaporated; and heating at 500 °C for 10 min	Polished with 0.3 μm[d] alumina powder; immersed for 30 s in mixture of concd H_2SO_4, 30% H_2O_2, and H_2O (3:1:1)

a) Ref. 15. b) Super pure CdS powder, *ca.* 1 g (Furuuchi Chemicals) pressed at 150 kg/cm² and sintered in N_2 atmosphere at 600—700 °C for 3 h. c) Y. Nakato, S. Tonomura, and H. Tsubomura, *Ber. Bunsenges. Phys. Chem.*, **80**, 1289 (1972). d) P.A. Kohl and A.J. Bard, *J. Electrochem. Soc.*, **126**, 603 (1979). e) ZnO powder, *ca.* 1 g (Wako Pure Chemical Industries) pressed at 150 kg/cm² and sintered at 1300 °C for 3 h. f) W.P. Gomes, T. Freund, and S. R. Morrison, *J. Electrochem. Soc.*, **115**, 818 (1968). g) Calculated by Motto-Schottky plots. h) Ref. 18.

($T\Delta S$) accompanied by oxidation of sulfite ions is exothermic, the correction value for the heat ($T\Delta S$) has the opposite sign as compared with the case of oxidation of $K_4Fe(CN)_6$.[4] Energy conversion efficiencies of various kinds of semiconductor photoelectrodes obtained by the photothermal measurement were reported.[14]

A straight line with a slope equal to 1.0 can be observed in the limiting photocurrent region (Fig. 4), indicating that the quantum efficiency of the oxidation of sulfite ions on the illuminated CdS single crystal electrode is unity as shown in Fig. 2.[4]

The results were obtained under the conditions where each parameter, E, I, t, is constant. The effects of various parameters on the quantum efficiencies (slopes) were checked at first, using the CdS–Na_2SO_3 and ZnO–Na_2SO_4 system.

Effect of Exciting Wavelengths. On usual semiconductor photoelectrodes, the quantum efficiencies are almost the same in the wavelength region shorter than that corresponding to the band gap energy.

Figure 5 shows the results of the effect of exciting wavelengths on the slope using the CdS–Na_2SO_3, where t and I are constant. The wavelengths of monochromatic light irradiated were 340, 400, and 490 nm. When 340 nm was used to excite the CdS electrode, the temperature increase measured at open circuit corresponded to $E=3.6$ eV. Three parallel straight lines were observed. Use of the shortest wavelength light gave a line located in the highest position, indicating that electrons excited into the conduction band move through radiationless processes to the bottom of the conduction band, giving rise to an increase in $Q_{s.c.}$. The fact that the slope was 1.0 in all cases indicates that quantum efficiency was 1.0 at all three wavelengths. Thus we could use light of any wavelength

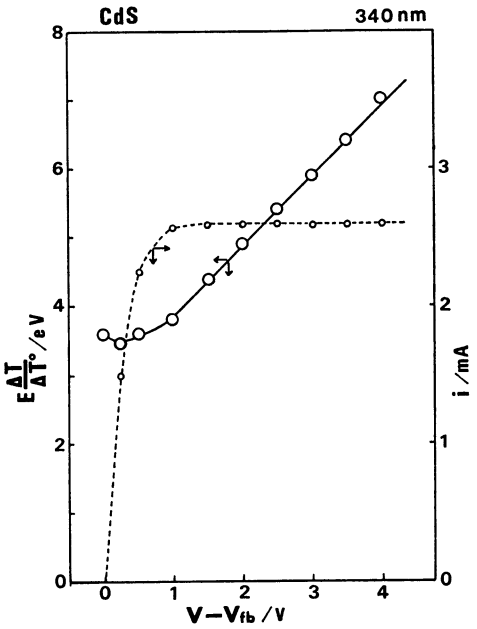

Fig. 4. Standardized temperature change *versus* potential from the flatband potential of the CdS single crystal electrode in 0.1 M Na_2SO_3 and 0.2 M Na_2SO_4.

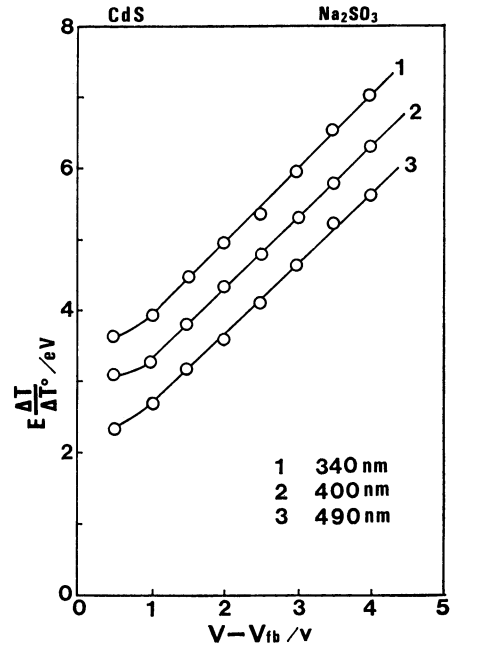

Fig. 5. The effect of exciting wavelengths on slope for the CdS single crystal electrode in 0.1 M Na_2SO_3 and 0.2 M Na_2SO_4.

shorter than that corresponding to the band gap energy to determine the quantum efficiency of a semiconductor reaction. If quantum efficiency changes with wavelengths, the slopes would also change.

Effect of Irradiation Time. The potential-ΔT relationship for the CdS–Na_2SO_3 system was measured at different irradiation times with light of constant intensity (photon numbers 5×10^{15} cm^{-2} s^{-1}), the slope being 1.0 in the irradiation time range 5—60 s (Fig. 6). A slope of 1.0 might be obtained even when irradiation

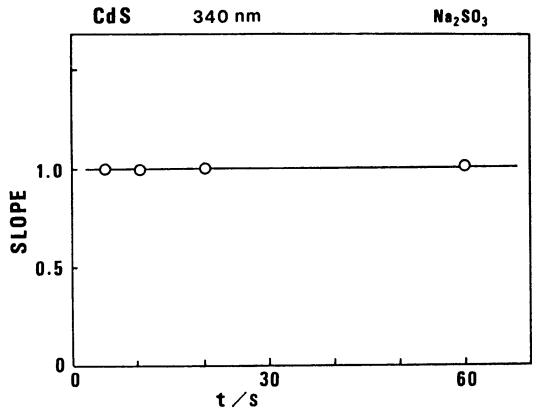

Fig. 6. The effect of irradiation time on slope for the CdS single crystal electrode in 0.1 M Na_2SO_3 and 0.2 M Na_2SO_4.

time is below 5 s. This was the case for 1.0 s irradiation time. However, in this case light of stronger intensity (1.8×10^{16} cm^{-2} s^{-1}) was introduced to the semiconductor surface to obtain a distinct rise in temperature. A slope can also be measured precisely by using a chopping system of light irradiation and a lock-in amplifier technique. When the semiconductor surface is excited for longer than 1 min (*e.g.* 2—5 min), the slope is expected to also be 1.0. However, in the irradiation time range 5—60 s, which we usually use, measurement is very easy.

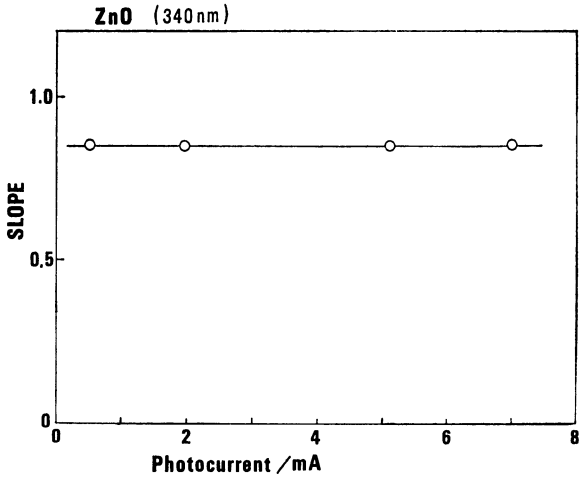

Fig. 7. The effect of light intensity on slope for the ZnO polycrystal electrode in 0.2 M Na_2SO_4.

Effect of Light Intensity. The effect of light intensity on the slope was studied using a polycrystal ZnO electrode in 0.2 M Na_2SO_4 (1 M=1 mol dm^{-3}) electrolyte solution. The results are shown in Fig. 7, where the abscissa represents the saturated photocurrent, which is proportional to the light intensity controlled by use of neutral density filters. The slope, *i.e.*, the quantum efficiency of the anodic reaction of the ZnO, was constant (0.85) at photocurrents of 500 μA cm^{-2}—7 mA cm^{-2} under the conditions of 340 nm wavelength and 20 s irradiation time (Fig. 7). The number of photons irradiated, as counted by chemical actinometry,

was between 4×10^{15}—6×10^{16} cm^{-2} s^{-1}. The magnitude of the photocurrent and the number of photons observed are of almost the same order as when measured in typical semiconductor electrode reactions.

The fact that these three parameters, *i.e.* wavelength, irradiation time, and intensity of light, can be appropriately selected depending on the characteristics of semiconductor electrodes indicates that this method is useful for obtaining quantum efficiencies.

n-Type Semiconductor Electrodes. CdS Single Crystal: As seen in the result for the CdS single crystal electrode, *i.e.* a slope of 1.0 (Fig. 4), oxidation of the sulfite ions occurs instead of dissolution of the CdS in a sodium sulfite solution.[15] On the other hand, quantum efficiency obtained by a comparison of the number of electrons calculated from the magnitude of photocurrent with the number of photons counted by chemical actinometry is 0.90—1.00, depending on the surface treatment.

CdS Polycrystal: The same reducing agent, SO_3^{2-}, was also used to suppress the dissolution of the polycrystal CdS electrode. The slope was 0.67, smaller than that of the single crystal CdS, probably due to the increase in surface recombination.

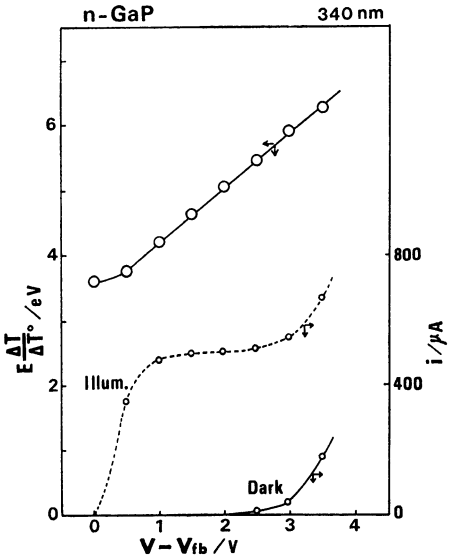

Fig. 8. Standardized temperature change *versus* potential and photocurrent *versus* potential of the n-GaP single crystal in 0.1 M Na_2S and 1 M NaOH.

n-CdSe, n-GaP, and n-GaAs Single Crystals: These semiconductor electrodes are also unstable in the usual electrolyte solution. For example, in 1 M NaOH, n-GaP dissolves under irradiation as follows:[16]

$$GaP + 11OH^- + 6p^+ \longrightarrow GaO_3^{3-} + HPO_3^{2-} + 5H_2O.$$

However, by using a strong reducing agent such as Na_2Se, the dissolution reactions can be suppressed.[17] Photothermal data and photocurrent-potential curves for the n-GaP electrode in a Na_2S aqueous electrolyte solution are shown in Fig. 8. Ellis *et al.*[17] reported that n-GaP was not stabilized perfectly in the Na_2S aqueous solution. However, we observed a constant photocurrent flow, indicating that the surface of the GaP electrode does not change during such a short irradiation period and weak intensity of light. The slope of $E\frac{\Delta T}{\Delta T^\circ}$ against potential was 0.85, which was larger than the quantum efficiency 0.62 obtained by chemical actinometry. In aqueous electrolyte solutions of the same reducing agent (Na_2S) the slope obtained for n-CdSe was 0.42 and that for n-GaAs 0.80. The value obtained for GaAs by chemical actinometry was considerably smaller (0.47). The large difference between the quantum efficiency from the slope and that from the chemical actinometry is not easy to interpret, since the surface of GaAs was not highly reflective as in the case of MoS_2.

TiO_2 Single Crystal: The slope, *i.e.* the quantum efficiency from temperature measurement, for TiO_2 changes with reduction treatment. By using TiO_2 single crystal reduced in a hydrogen atmosphere at 600 °C for 20 min, we obtained a slope of 0.7 in an aqueous solution of sulfuric acid.

ZnO Polycrystal: The results are shown in Fig. 7. The quantum efficiency from the slope is 0.85.

n-MoS_2 Single Crystal: For lustrous semiconductors, it is difficult to estimate the quantum efficiency of the photoelectrode reaction by the usual method of counting the number of photons by chemical actinometry. By the temperature method, we count only the photons absorbed in the surface of the semiconductor, with the result that value thus obtained for quantum efficiency can be taken as an intrinsic quantum efficiency. One of the most lustrous semiconductors is MoS_2, known as a layer compound semiconductor. Tributsch[18,19] reported that n-MoS_2 is a most promising photoelectrode for the electrochemical photocell because of its wide wavelength spectrum for photoactive reactions. Figure 9 shows the results with an n-type MoS_2 electrode. Under irradia-

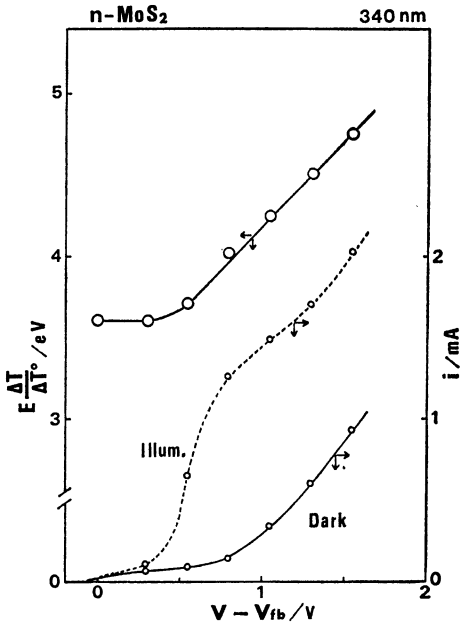

Fig. 9. Standardized temperature change *versus* potential and photocurrent *versus* potential of the n-MoS_2 single crystal in 0.2 M Na_2SO_4.

tion the limiting anodic photocurrent was obtained by substracting the anodic dark current. The slope of $E\frac{\Delta T}{\Delta T^{\circ}}$ due to a saturated photocurrent against the applied potential was 1.0. On the other hand, the quantum efficiency from the usual actinometric method was 0.54, suggesting that the temperature method is useful to determine the intrinsic quantum efficiency of a semiconductor electrode with a brilliant surface.

p-Type Semiconductor Electrodes. p-GaP and p-GaAs Single Crystal: In p-type semiconductor electrodes, the cathodic current increases by light irradiation. In the cathodic limiting photocurrent region, the relationship between temperature change and the applied potential can also give information on the intrinsic quantum efficiency. Figure 10 shows the results for a p-GaP single crystal electrode. From the linear slope, it was possible to obtain the intrinsic quantum efficiency of 0.80 for the hydrogen evolution reaction.

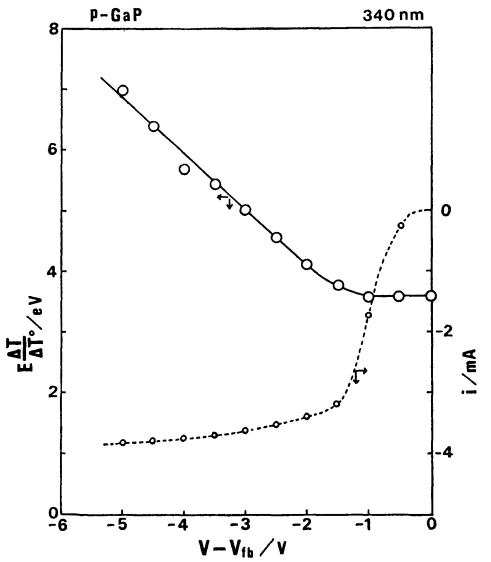

Fig. 10. Standardized temperature change *versus* potential and photocurrent *versus* potential of the p-GaP single crystal in 0.5 M H_2SO_4.

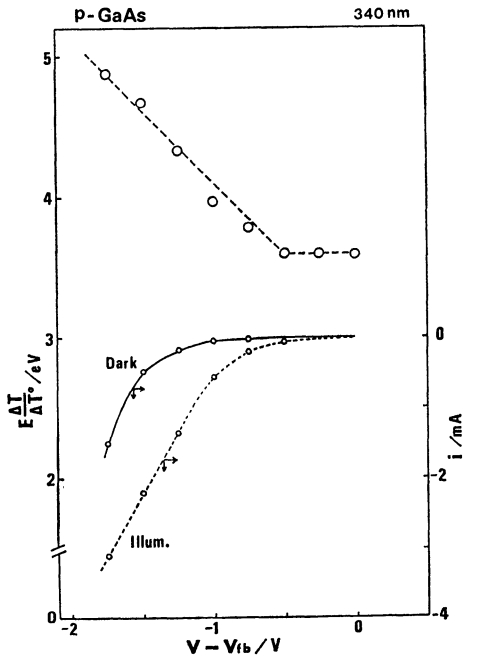

Fig. 11. Standardized temperature change *versus* potential and photocurrent *versus* potential of the p-GaAs single crystal in 0.5 M H_2SO_4.

Figure 11 shows the results for a p-GaAs single crystal electrode. Even in the limiting photocurrent region, the cathodic photocurrent increases gradually with cathodic polarization, the $E\frac{\Delta T}{\Delta T^{\circ}}$ *vs.* V curve showing no straight line. In this case, the slope of the tangent of the curve might indicate the quantum efficiency. Even in actinometric method, the quantum efficiencies showed different values depending on the applied potential, since the photocurrent is dependent on the applied potential in spite of the constant number of photons irradiated.

Summary

A comparison is made of the intrinsic quantum efficiencies obtained from the temperature measurement of the semiconductor surfaces (Table 2).

Table 2. Comparison of quantum efficiencies

340 nm

Electrode	η_t	η_a	Electrolyte
n-CdS s	1.00	1.00	Na_2SO_3
n-CdS p	0.67	0.67—0.70	Na_2SO_3
n-CdSe s	0.42	0.40—0.42	Na_2S
n-GaP s	0.85	0.62	Na_2S
n-GaAs s	0.80	0.47—0.49	Na_2S
n-TiO_2 s	0.70	0.70	H_2SO_4
n-ZnO p	0.85	0.76—0.78	Na_2SO_4
n-MoS_2 s	1.00	0.54	Na_2SO_4
p-GaP s	0.80	0.60—0.66	H_2SO_4
p-GaAs s	0.80—1.00	0.56—0.59	H_2SO_4

η_t:Quantum efficiency by temperature measurement.
η_a:Quantum efficiency by actinometry. s: Single crystal.
p: Polycrystal.

This temperature method has advantages over the usual actinometric method; i) simplicity, ii) no necessity of counting the number of photons irradiated and/or absorbed, iii) the possibility of obtaining intrinsic quantum efficiencies even for semiconductors which have large surface reflectance and/or scattering.

References

1) G. H. Brilmyer, A. Fujishima, K. S. V. Santhanam, and A. J. Bard, *Anal. Chem.*, **49**, 2057 (1977).
2) A. Fujishima, H. Masuda, K. Honda, and A. J. Bard, *Anal. Chem.*, **52**, 682 (1980).
3) G. H. Brilmyer and A. J. Bard, *Anal. Chem.*, **52**, 685 (1980).
4) A. Fujishima, Y. Maeda, K. Honda, G. H. Brilmyer, and A. J. Bard, *J. Electrochem. Soc.*, **127**, 840 (1980).
5) A. Fujishima and K. Honda, *Nature*, **283**, 37 (1972).

6) A. Fujishima, K. Kohayakawa, and K. Honda, *J. Electrochem. Soc.*, **122**, 1487 (1975).
7) H. Gerischer, *J. Electroanal. Chem.*, **58**, 263 (1975).
8) A. J. Bard, *J. Photochem.*, **10**, 59 (1979).
9) A. B. Ellis, S. W. Kaiser, and M. S. Wrighton, *J. Am. Chem. Soc.*, **98**, 6855 (1976).
10) B. A. Parkinson, A. Heller, and B. Miller, *J. Electrochem. Soc.*, **126**, 954 (1979).
11) A. Fujishima, G. H. Brilmyer, and A. J. Bard, "Semiconductor-Liquid Junction Solar Cells," ed by A. Heller, Electrochemical Society, Inc., Princeton, N. J. (1977), Proceeding Vol. 77-3, pp. 172—176.
12) C. G. Hatchard and C. A. Parker, *Proc. R. Soc. London, Ser. A*, **235**, 518 (1956).
13) R. Tamamushi, *J. Electroanal. Chem.*, **45**, 500 (1973); **65**, 263 (1975).
14) Y. Maeda, A. Fujishima, and K. Honda, *Rev. Polarogr.*, **24**, 87 (1978).
15) T. Inoue, T. Watanabe, A. Fujishima, K. Honda, and K. Kohayakawa, *J. Electrochem. Soc.*, **124**, 719 (1977).
16) K. Kohayakawa, A. Fujishima, and K. Honda, *Nippon Kagaku Kaishi*, **1977**, 780.
17) A. B. Ellis, J. M. Bolts, S. W. Kaiser, and M. S. Wrighton, *J. Am. Chem. Soc.*, **99**, 2848 (1977).
18) H. Tributsch and J. C. Bennett, *J. Electroanal. Chem.*, **81**, 97 (1977).
19) H. Tributsch, *Ber. Bunsenges. Phys. Chem.*, **81**, 361 (1977).